A Real-Time Four-Dimensional Doppler Dealiasing Scheme

CURTIS N. JAMES* AND ROBERT A. HOUZE JR.

Department of Atmospheric Sciences, University of Washington, Seattle, Washington

(Manuscript received 26 June 2000, in final form 23 April 2001)

ABSTRACT

A new dealiasing scheme uses the full four-dimensionality available in an operational Doppler radar data stream. It examines one tilt angle at a time, beginning at the highest elevation where clutter is minimal and gate-to-gate shear is typically low compared to the Nyquist velocity. It then dealiases each tilt in descending order until the entire radial velocity volume is corrected.

In each tilt, the algorithm performs six simple steps. In the first two steps, a reflectivity threshold and filter are applied to the radial velocity field to remove unwanted noise. The third step initializes dealiasing by attempting to adjust the value of each gate by Nyquist intervals such that it agrees with both the nearest gate in the next higher tilt and the nearest gate in the previous volume. The gates that pass the third step at a high confidence level become the initial values for step four, which consist of correcting the neighboring gates within the scan, while preserving environmental shear as much as possible. In step five, remaining gates are compared to an average of neighboring corrected gates, and anomalous gates are deleted. As a last resort, step six uses a velocity azimuth display (VAD) analysis of the wind field to interpret and correct any remaining isolated echoes.

This scheme uses all available data dimensions to interpret and dealias each tilt and is efficient enough to operate on a continuous data stream. It performs reliably even in difficult dealiasing situations and at low Nyquist velocity. During two complex events observed by low-Nyquist Doppler radar in the European Alps, 93% of 4300 tilts were dealiased without error. When errors did occur, they were usually confined to small regions and most frequently resulted from the occurrence of gate-to-gate shear that was impossible to resolve by the Nyquist velocity.

1. Introduction

During the 1999 Mesoscale Alpine Programme (MAP; Binder et al. 1995; available online at www.map.ethz.ch; Bougeault et al. 2001), a ground-based Doppler radar array was configured to deduce the microphysical structure and three-dimensional wind field of precipitating systems over the southern slopes of the European Alps. According to Georgis et al. (2000), it was the third meteorological experiment ever conducted in complex terrain that provided multiple-Doppler observations, and only the second to focus on the evolution of the three-dimensional wind field over topography. More importantly, it was the first project of this type to produce three-dimensional Doppler radar syntheses of the mesoscale wind in real time (Chong et al. 2000; syntheses available online at www.joss.ucar.edu/map/catalog/). These syntheses could not have been achieved without first removing aliasing error from the radial velocity fields by efficient, automatic dealiasing algorithms.

Aliasing occurs when the radar's pulse repetition frequency (PRF) is too low to resolve the phase shift $\Delta\phi$ that occurs between successive pulses reflected by moving precipitation particles. This phase shift may be expressed as

$$\Delta\phi = \frac{4\pi V_r}{\lambda \mathrm{PRF}}, \tag{1}$$

in which λ is the radar wavelength and V_r is the radial component of the target's velocity [see Houze (1993) for further discussion]. The discrete sampling of the phase of reflected waves at a fixed time interval (or PRF) means that the true phase shift $\Delta\phi$ can never be known with certainty. The apparent phase shift detected by the radar may differ from the true $\Delta\phi$ by plus or minus some integer multiple of 2π. This circumstance is called aliasing. The maximum target velocity that will produce no aliasing is called the Nyquist velocity and is given by

$$V_n = \frac{\lambda \mathrm{PRF}}{4}. \tag{2}$$

* Current affiliation: Meteorology Lab, Embry-Riddle Aeronautical University, Prescott, Arizona.

Corresponding author address: Professor R. A. Houze Jr., Department of Atmospheric Sciences, Box 351640, University of Washington, Seattle, WA 98195-1640.
E-mail: houze@atmos.washington.edu

The apparent radial velocity V_a (assuming no aliasing) depends on V_r and V_n as

$$V_a = V_r + 2nV_n, \tag{3}$$

where n is an unknown integer (positive or negative).

Dealiasing (often called unfolding) is the process of determining n at each radar gate such that the true radial velocity field (V_r) is retrieved from the apparent radial velocity field (V_a). In operational meteorology and in field research, dealiasing must be achieved automatically because of the vast quantity of radar data received in a given time interval. Dealiasing algorithms developed prior to this study have used either one-dimensional (radial) or two-dimensional (radial and azimuthal) continuity constraints to remove folds. Provided that an initial value of V_r is obtained at one of the gates in each contiguous data region, these schemes adjust V_a at the remaining gates by multiples of $2V_n$ to minimize gate-to-gate shear and retrieve V_r. Thus, dealiasing is similar to solving an initial value problem, where first-order derivatives are integrated over some interval and added to a specified initial value.

The efficacy of a dealiasing algorithm depends on radar characteristics and environmental conditions. In high wind events, and at low V_n, multiple folds lead to poor performance of the algorithm. When the gate-to-gate shear is poorly resolved by V_n, it is difficult and sometimes impossible to retrieve V_r. Stratiform precipitation echoes are more continuous and therefore easier to dealias than are convective echoes.

In orographic precipitation, dealiasing is particularly difficult. Convective initiation is common over orography (Banta 1990). The influence of mountains on the atmosphere results in a myriad of complex flow phenomena such as flow blocking, barrier jets, downslope flow, vorticity generation, and local wind systems (Smith 1979; Durran 1986; Schär and Durran 1997; Whiteman 1990). These effects produce horizontal and vertical shears that complicate dealiasing. When radar beams encounter mountains, low-valued velocities result, which, if not removed, can be misinterpreted by dealiasing algorithms during strong wind events. Beam blockage also splits single precipitation systems into multiple radar echoes, further complicating the dealiasing problem.

An algorithm's performance also strongly depends on its design and the characteristics of the radar to which it is applied. Two important features that differentiate the existing dealiasing algorithms are the method used to produce initial values in each contiguous data region and the algorithm's ability to remove aliasing within that region in spite of strong shear, noise, and clutter. In preparing for MAP, we found that the existing dealiasing schemes did not work well for the Swiss Meteorological Agency's Monte Lema radar (Joss et al. 1998). This radar operates with a particularly small Nyquist velocity of 8.27 m s^{-1} in the lowest tilts over the mountainous terrain. The resulting severe aliasing problems led us to develop a more comprehensive dealiasing scheme, which uses the full four-dimensionality of an operational Doppler-radar data stream to remove aliasing error. The purpose of this paper is to describe this powerful new dealiasing method and present the four-dimensional dealiasing algorithm.

2. Previous dealiasing algorithms

The first dealiasing algorithms were one-dimensional schemes using only radial information to diagnose and remove folds. Ray and Ziegler (1977) required that the gates in all or part of a radial be normally distributed about their mean. They adjusted outlying gates by multiples of n. This technique can be effective only when the data are well approximated by a Gaussian distribution and only minor aliasing occurs.

Bargen and Brown's (1980) one-dimensional scheme used spatial continuity along each radial to remove local folds. They assumed that the first gate in each radial was free of error. They compare successive gates in the radial with averages of previously dealiased gates in the radial to evaluate the number of folds at each gate. However, strong wind events tend to violate the first-gate assumption. Their scheme therefore permits user intervention such as specifying an initial velocity, the number of preceding gates to include in the running average, or the dealiasing direction (i.e., radially away from or toward the radar and azimuthally clockwise or counterclockwise). The user is also permitted to edit the data. Nevertheless, user intervention is not feasible for real-time applications or very large datasets. In addition, Eilts and Smith (1990) suggest that one-dimensional continuity schemes cannot unambiguously dealias shear zones without incorporating other data dimensions.

Hennington's (1981) algorithm incorporated a vertical wind profile from a nearby sounding to calculate the radial component of the environmental wind field V_{env}. In this approach, n is determined using the expression

$$n = \text{nint}\left(\frac{V_{\text{env}} - V_a}{2V_n}\right), \tag{4}$$

in which nint is a function that returns the nearest integer. However, this equation assumes that V_r falls within the range $\pm 2V_n$, which is unreasonable for radars with low V_n or during high wind events. Hennington's use of an environmental sounding neglects horizontal shear and requires the availability of a nearby sounding or wind profile. In addition, it fails to incorporate data continuity between adjacent radar gates to diagnose and remove aliasing.

Most dealiasing algorithms developed since the early 1980s have implemented spatial continuity constraints as well as some general information about the wind field. Thus they have combined the approaches of Bargen and Brown (1980), Hennington (1981), and others. The operational Weather Surveillance Radar-1988

Doppler (WSR-88D) algorithm (Eilts and Smith 1990) uses a vertical wind profile from an environmental sounding to produce initial values for each elevation scan and for isolated echoes. Otherwise, the scheme applies radial continuity constraints to remove local aliasing error and azimuthal continuity checks to mitigate error. The scheme also incorporates radial averages to determine n when continuity thresholds are not met. Thus, the scheme incorporates both supplemental wind information and two-dimensional continuity. It is efficient and has proven highly effective over the Great Plains for V_n values between 20 and 35 m s^{-1}.

Merritt (1984) developed a wind-field model technique that uses the radial velocity field around an azimuth circle to determine the wind direction. The wind model, which is allowed to vary with height while neglecting horizontal shear, helped to interpret isolated echoes. Bergen and Albers (1988) expanded Merritt's scheme using WSR-88D velocity azimuth display (VAD) wind profiles (Browning and Wexler 1968) to include the magnitude of the wind as well as the direction. They found that VADs were adequate to resolve isolated data; however, their algorithm tests were performed for weak horizontal shear and with Nyquist velocities greater than or equal to 17 m s^{-1}. Bergen and Albers also experimented with a three-dimensional dealiasing approach. They tested several volume scans using vertical continuity from tilt to tilt to provide additional information to dealias isolated areas. They found that the three-dimensional technique performed just as well as the two-dimensional technique, and it reduced the need for auxiliary wind information from a VAD.

Jing and Wiener (1993) developed a sophisticated two-dimensional algorithm that solved a linear system that minimized gate-to-gate shear in each isolated echo. This technique assumes a smooth environmental wind field with weak shear and compares each locally dealiased echo to an environmental wind field estimate or VAD wind profile. The calculated average is then minimized by incrementing n equally over the entire echo. Jing and Wiener also assume that the average local wind observed by radar is less than V_n.

Yamada and Chong (1999) produced an algorithm that first locates the azimuth circle in each tilt that contains the largest number of valid velocity gates. Azimuthal continuity-based dealiasing is then applied, and the VAD from the single azimuth circle is fitted to a second-order Fourier series. The zero-order Fourier coefficient is incremented by Nyquist intervals (i.e., multiples of $2V_n$) to retrieve V_r over the entire azimuth circle, which can subsequently be used to correct adjacent gates in the tilt. Unfortunately, this approach is only satisfactory when the available data coverage is high, the noise level is low, nonlinear wind components are negligible, and the Nyquist velocity is high.

Although dealiasing schemes have progressed significantly, none prior to the present study utilizes the full four-dimensionality now available in most operational Doppler data streams. Instead, they rely heavily on auxiliary wind information such as soundings, wind models, or VADs. In various degrees, the schemes therefore fail to capture the full complexity of the wind field. They neglect horizontal wind shear, which is an important consideration during severe events and in complex terrain. Furthermore, few of these algorithms have been tested at low V_n (i.e., less than 15 m s^{-1}) where the dealiasing problem is particularly challenging, or over complex orography.

3. Description of four-dimensional dealiasing (4DD)

a. General philosophy and approach

Bergen and Albers (1988) suggested that adding the vertical dimension to a two-dimensional dealiasing scheme more accurately interprets the environmental wind field and diminishes an algorithm's requirements for auxiliary wind information. This reasoning can be extended to include the fourth dimension: *time.* We have developed four-dimensional dealiasing (4DD); a scheme that utilizes the four-dimensionality currently available with most operational Doppler data streams. 4DD was developed for and successfully used in real-time operation during MAP. It performed well in a highly sheared orographic regime at low V_n.

4DD also requires auxiliary wind information, but its dependence on this information is greatly reduced using the time dimension. In a series of radar volumes, the best approximation to the radial velocity field in a given volume is probably the velocity field of the previous radar volume as long as that field has been properly dealiased. Using the vertical dimension can also greatly improve dealiasing algorithm performance. Since operational radars usually employ higher PRFs at higher tilt angles, dealiasing is less difficult in the higher tilts. Noise, clutter, and wind shear also typically diminish with height, and higher tilts are therefore a valuable resource for dealiasing adjoining lower tilts. In addition to vertical and temporal continuity, 4DD uses both radial and azimuthal dimensions to interpret shear zones. Continuity constraints are also applied between gates that share the same corner, that is, that are *diagonally* adjacent, thus further removing ambiguities caused by environmental shear.

Although 4DD uses all available data dimensions plus auxiliary wind information, the algorithm's construction is simple and straightforward (Fig. 1). Processing begins by reading into memory both the current radial velocity volume (CVR) and, if available, the previously dealiased radial velocity volume (PDVR). Other algorithm inputs include the reflectivity field (DZ) and an environmental wind profile from a VAD analysis or sounding. The environmental wind data are loaded one height level at a time, beginning at low levels where VAD winds are typically more reliable. Then, as each level is loaded in succession, a vertical shear check is per-

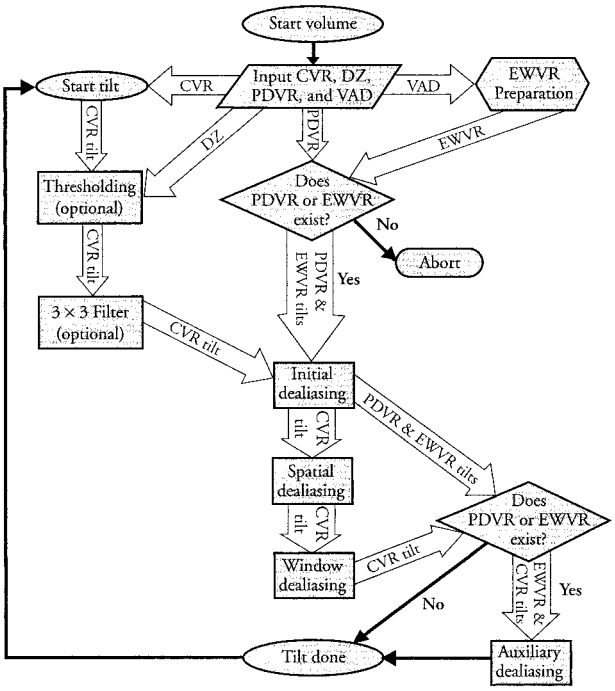

FIG. 1. Flowchart depicting the processing chain performed on each radar volume by 4DD.

formed between the previous level and the current level. The current wind vector is deleted if the magnitude of the shear exceeds a user-specified threshold (default $>$ 0.05 s^{-1}). The removal of strong vertical shear removes potentially erroneous winds and strong small-scale variability in the environmental wind profile. Once all levels are loaded that fall within the required shear threshold, the wind is linearly interpolated and the radial velocity field is estimated for each radar gate assuming standard atmospheric refraction (e.g., Doviak and Zrnić 1993) and negligible horizontal shear. The result is a smoothed, synthetic radial velocity field (hereafter EWVR).

After loading PDVR, EWVR, and CVR into memory, the algorithm examines CVR tilt by tilt, starting at the highest elevation where clutter is minimal and gate-to-gate differences in radial velocity are typically small compared to the Nyquist velocity. It then dealiases the lower tilts in descending order until the entire radial velocity volume is corrected. The algorithm performs six basic steps in each tilt: thresholding, filtering, initial dealiasing, spatial dealiasing, window dealiasing, and auxiliary dealiasing. A description of these six steps follows.

b. Thresholding

When the signal-to-noise ratio (SNR) is low, radar measurements are more affected by clutter, second-trip echoes, and other errors. Bergen and Albers (1988) note that low SNR gates should be removed prior to dealiasing to improve an algorithm's efficiency and to remove artificial gradients that can be misinterpreted as aliasing error. Bargen and Brown (1980) suggest thresholding as one possible way to remove noise. Prior to dealiasing, 4DD deletes all radial velocity gates in which the reflectivity falls outside of a user-specified valid range (default 0–80 dBZ). Another input parameter allows the user to delete a radial velocity gate when the corresponding reflectivity value is missing. As a result of the dBZ thresholding, many of the low SNR returns are removed. A more robust approach would be to threshold on raw power, spectral width, and/or normalized coherent power measurements; however, these fields are often not available in real-time operational data streams.

c. Filtering

Following data thresholding, a simple and computationally efficient Bergen and Albers (1988) filter is applied to remove isolated gates. Depending on the dealiasing algorithm, Bergen and Albers claim that the 3 $\times$ 3 filter can improve algorithm efficiency by a factor of 5 or more. Each gate within the radar tilt that contains a valid radial velocity value is considered. If more than three of its eight neighboring gates are missing, it is assigned a missing value flag and eventually deleted. A second pass through the tilt then deletes any remaining gates in which all of the neighboring gates have been removed. This technique removes isolated points as well as questionable velocities in ''speckled'' regions (usually between 2% and 4% of the velocity gates are deleted). In good data regions, the filter effectively preserves echo boundaries and shapes, although a few of the gates that form sharp echo boundaries are removed [see Bergen and Albers (1988) for more details].

d. Initial dealiasing

Following thresholding and filtering, initial dealiasing is performed. Initial dealiasing is performed in each tilt using temporal and vertical continuity and is based on a simple scaling argument. For typical mesoscale flow resolved by Doppler radar, the local time rate of change of wind velocity $\partial\mathbf{V}/\partial t$ scales as

$$\frac{U^2}{L} \sim \frac{(10 \text{ m s}^{-1})^2}{10^3 \text{ m}} = 0.01 \text{ m s}^{-1}. \quad (5)$$

Since $|V_r| \leq |\mathbf{V}|$,

$$\left|\frac{\Delta V_r}{\Delta t}\right| \sim 0.01 \text{ m s}^{-1} \quad \text{or less}, \quad (6)$$

where Δt is the time interval between consecutive radar volumes. Therefore, neglecting measurement error and noise, the change in the true radial velocity between successive volumes ΔV_r is on the order of 3 m s^{-1} or less for a 5-min volume scan.

PDVR is therefore a good estimate of CVR, as long

as V_n is larger than ΔV_r, and it is generally possible to dealias CVR against the PDVR. Unfortunately, such a simple time continuity constraint, when used alone, allows errors in the previous volume to pass into the current volume and propagate indefinitely through the data stream. In addition, measurement error, noise, strong wind shear, and strong accelerations can produce large ΔV_r values that are not well resolved by V_n and generate new errors.

To mitigate the development and propagation of error, 4DD uses the vertical dimension along with the time dimension to constrain initial dealiasing. Only those gates in CVR that can be dealiased to within $0.25V_n$ of the same gate in PDVR *and* $0.25V_n$ of the nearest gate in the previous tilt above are considered correctly dealiased. These gates are saved and assigned a ''good'' flag; all others are left unaltered. This routine produces a number of gates scattered throughout the tilt that are dealiased to a high degree of confidence and that serve as initial-value gates for spatial dealiasing.

If PDVR is unavailable (i.e., dealiasing is being initialized on the first of a series of volumes), EWVR is used in its place. Since EWVR is generated using a VAD or sounding (neglecting horizontal shear), dealiasing is typically more problematic in the first few volumes in a sequence. Ordinarily it should not be necessary to reinitialize dealiasing as long as the data flow is uninterrupted by radar outages or communication problems.

e. Spatial dealiasing

In spatial dealiasing, good initial-value gates are used to dealias adjacent gates spatially within the tilt. Each gate that borders a good gate is adjusted by an integer n such that it agrees with all of its neighboring good gates (maximum eight) within a gate-to-gate shear threshold[1] of $0.4V_n$. If this procedure is successful, the value of the current gate in question is saved, flagged as good, and used to dealias other gates. Otherwise, it is assumed that noise or shear has been encountered and the algorithm saves the gate for future passes, thus allowing the algorithm to postpone problem gates until more good gates are available to interpret them. Postponing these difficult gates makes dealiasing more robust in high-shear regions. In addition, errors that more commonly originate in high-shear regions are confined to smaller areas since the surrounding gates are dealiased first.

During the first spatial dealiasing pass, 4DD scans outward along each radial and progresses radial by radial in a clockwise direction. During each successive pass, 4DD alternates between clockwise and counterclockwise progression while continuing to scan radially outward. The purpose for employing alternating directions is to improve algorithm efficiency and to allow 4DD to dealias around shear zones and problem areas during the first two passes. During the third pass, the threshold is relaxed to $1.0V_n$ and each gate must now agree with only a majority of the neighboring good gates, rather than all of them, for dealiasing to be considered successful. Thus, spatial dealiasing begins to interpret the more difficult regions during its third pass through each tilt and continues until completing a total of 10 passes or until the number of remaining gates with adjacent good gates decreases to zero.

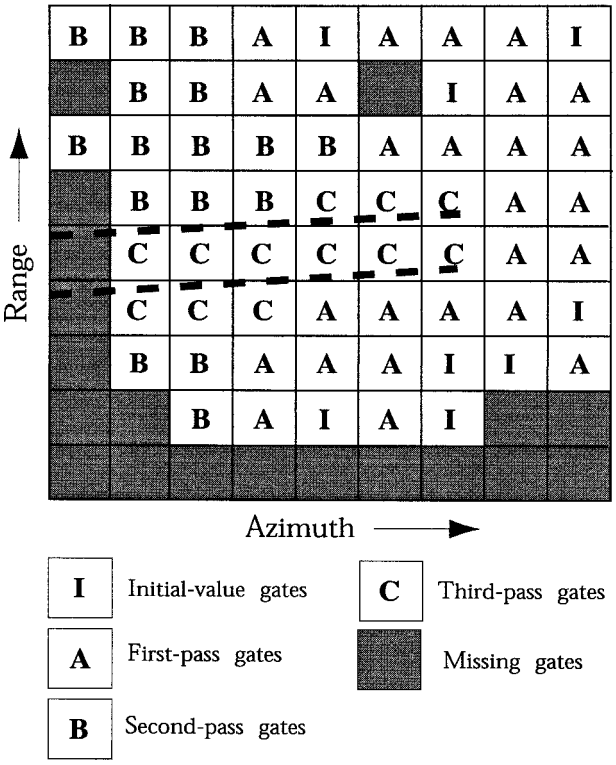

FIG. 2. The behavior of the spatial dealiasing routine illustrated within a hypothetical 9 × 9 azimuth–range sector. The heavy dashed lines indicate the boundaries of a shear zone with gate-to-gate shears greater than $0.4V_n$. All initial-value gates (i.e., those dealiased during initial dealiasing that are available as initial values for spatial dealiasing) are labeled ''I.'' Gates that are dealiased during the first, second, and third spatial dealiasing passes are denoted ''A,'' ''B,'' and ''C,'' respectively. It should be noted that spatial dealiasing scans radially outward in clockwise (counterclockwise) order during the first and third passes (second pass), and that the shear threshold is relaxed from $0.4V_n$ to $1.0V_n$ before the third pass.

Figure 2 illustrates the behavior of the spatial dealiasing routine in a hypothetical range–azimuth sector. In this example, it is assumed that the gate-to-gate shear is less than $0.4V_n$ over the entire sector except between the two thick dashed lines. The initial-value gates (i.e., those that were dealiased by the initial dealiasing routine) are labeled ''I'' in the figure. During the first spatial dealiasing pass, 4DD scans outward along each radial in clockwise order (left to right in Fig. 2), incrementing each available uncorrected gate by Nyquist intervals until its value falls within $0.4V_n$ of any adjacent initial-

[1] The threshold value 0.4 was obtained through preliminary tests of 4DD. Threshold values greater than 0.4 produced more frequent errors, while lower values decreased algorithm efficiency.

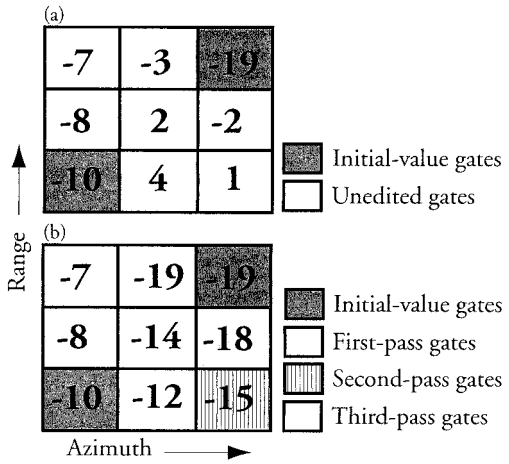

FIG. 3. Radial velocity values within a hypothetical 3 × 3 radar echo (a) before and (b) after executing the spatial dealiasing routine. In (a) initial-value gates are shaded, while uncorrected gates are not. In (b) initial-value gates are shaded as in (a), while gates corrected during the first, second, and third spatial dealiasing passes contain gradually lighter shading to none.

value gate or previously corrected gate. If successful, the value is saved and used to dealias other gates. If unsuccessful, the gate is left unchanged and is examined during subsequent spatial dealiasing passes. In the sample range–azimuth sector (Fig. 2), a number of gates are successfully corrected during the first pass (labeled ''A''). However, it is important to note that some gates within the first four radials remain uncorrected after the first pass simply because the radials are examined in clockwise succession. Other gates remain because they lie within the shear zone (between the dashed lines) where the gate-to-gate shear exceeds the $0.4V_n$ threshold.

4DD then performs a second spatial dealiasing pass in a manner identical to the first, except that the radials are examined in counterclockwise succession. By alternating the order in which the radials are examined, most of the remaining gates (labeled ''B'' in Fig. 2) are successfully dealiased during the second pass. Without alternating from clockwise to counterclockwise between successive passes, additional spatial dealiasing passes would be required to achieve the same result, and the algorithm's efficiency would be significantly less.

After the second pass, only those gates located within the shear zone remain uncorrected (labeled ''C''). These remaining gates are more easily dealiased during the third and subsequent passes, now that corrected gates are available on both sides of the shear zone and the gate-to-gate shear threshold is relaxed to $1.0V_n$. This example demonstrates how 4DD is more forgiving of strong gate-to-gate shear than other algorithms and approaches problem-dealiasing regions from all sides. This ability of the algorithm to save the most difficult dealiasing until the end reduces the areal extent of errors when they occur and is analogous to the way a trained observer would treat a difficult dealiasing problem.

TABLE 1. 4DD's test performance (3 and 5 Sep 1998).

Statistic	Result
Total volumes dealiased	241
Number of volumes returned with error	134
Average number of tilts per volume with error	1.27
Average number of isolated echoes deleted per volume	0.25
Total number of tilts containing valid data	4300
Number of tilts with aliasing	2414
Number of tilts containing valid data returned without error	3993
Number of tilts containing valid data returned with error	307
For the most problematic tilt in each volume	
Average percentage of tilt area with error	3%
Average percentage of valid data area with error	10%

Figure 3 illustrates 4DD performance in more detail. Figures 3a and 3b, respectively, depict the radial velocity field within a hypothetical 3 × 3 gate radar echo before and after spatial dealiasing. In this example, we assume that the Nyquist velocity is 8 m s^{-1} and that only two of the nine gates have passed initial dealiasing as initial-value gates (shaded gates, Fig. 3a). During the first pass of the spatial dealiasing routine, 4DD first examines the left radial. The second and third gates are considered good because the gate-to-gate shear between successive gates is less than $0.4V_n$ (or 3.2 m s^{-1}). However, the middle radial is left uncorrected during the first pass because none of the three gates in the radial can be adjusted by Nyquist intervals (16 m s^{-1}) such that their values fall within 3.2 m s^{-1} of their adjacent good gates. In the third radial, the second gate is corrected by adjusting its value by −16 m s^{-1} such that it differs from the adjacent initial-value gate by only 1 m s^{-1}. Thus three gates are corrected during the first pass (medium shading, Fig. 3b).

The algorithm then proceeds into the second spatial dealiasing pass, which examines the right radial first. It is found that by adjusting the first gate in that radial by one Nyquist interval, its value becomes −15 m s^{-1} (pinstripe, Fig. 3b), which falls within $0.4V_n$ of the adjacent gate that was corrected during the previous pass (−18 m s^{-1}). The algorithm then scans the middle radial, but leaves all three gates in the radial uncorrected since none of them can be adjusted to agree with all their adjacent good gates within $0.4V_n$. Only during the third pass is the middle radial dealiased, because now the threshold is relaxed to $1.0V_n$ (8 m s^{-1}), and each gate is required to agree with only a majority of its adjacent gates. In Fig. 3b, it appears that dealiasing was properly achieved, yet ambiguities result when the magnitude of the gate-to-gate shear exceeds the Nyquist velocity, such as between the left and middle radials. In some high-shear cases, the true radial velocity field becomes impossible to retrieve, despite the fact that 4DD's use of multiple data dimensions is forgiving of strong shear.

f. Window dealiasing

Following spatial dealiasing, many gates may remain uncorrected because they are not directly adjacent to

groups of corrected gates. Prior to incorporating auxiliary wind information from a VAD or sounding, a windowing step is performed because a local average of good velocity gates is likely to be a better estimate of the wind at a given gate than EWVR. During window dealiasing, 4DD scans through the gates that still remain to be corrected. Each gate is compared to the average value of all good gates within a centered azimuth–range window[2] of dimensions 11 × 11. If the population of good gates within the window equals or exceeds 5, then their collective mean and standard deviation are computed; otherwise, the window is expanded to 21 × 21. If the population of the enlarged window is still too small, the central gate is saved for the auxiliary dealiasing routine. Otherwise, the central gate is adjusted by increments of $2V_n$ until its value falls within $\pm V_n$ of the population mean. If the standard deviation is less than a specified threshold and the gate in question can be adjusted to within $0.7V_n$ of the mean, then the value is returned; otherwise, it is deleted because of the data scatter in the vicinity of the gate. Gates with low scatter and in close agreement (within $0.4V_n$) with the population mean are flagged as good and used to dealias other gates. 4DD tests indicate that a standard deviation threshold of approximately $0.8V_n$ generally works well.

g. Auxiliary dealiasing

After windowing, isolated echoes within the tilt may remain uncorrected. If new echoes have developed or moved within the range of the radar, initial dealiasing fails to interpret them using temporal and vertical continuity. In regions where valid data are unavailable in the adjoining tilt above, initial dealiasing also fails. Some echoes may fail the initial dealiasing step simply because the radial velocity values deviate from corresponding gates in the previous volume and the adjacent tilt. As a last resort, these echoes must therefore be initialized using auxiliary wind information.

If auxiliary wind information (EWVR) is unavailable, auxiliary deliasing obviously cannot be performed. If PDVR is unavailable, EWVR is used as a substitute for PDVR during initial dealiasing, and it is therefore not necessary to use EWVR again during auxiliary dealiasing. Therefore, the auxiliary dealiasing routine is performed only if both PDVR and EWVR are available. During auxiliary dealiasing, an attempt is made to initialize each gate within the remaining uncorrected echoes by comparing it with the corresponding gate in EWVR. If its value can be adjusted by Nyquist intervals such that it agrees to within $0.5V_n$ of EWVR, the velocity gate is saved, and a good flag is assigned. After the isolated echoes are initialized using EWVR, spatial dealiasing ensues within each echo.

[2] In order to maintain algorithm simplicity and efficiency, window dealiasing considers azimuth–range windows rather than geographic areas.

TABLE 2. Leading causes of error by volume (3 and 5 Sep 1998).

Leading cause of improper dealiasing	No. of volumes	Percent of total (134)
Unresolved shear:	73	54%
Horizontal shear	40	30%
Strong turbulence	25	19%
Vertical shear	8	6%
Echoes incorrectly interpreted (using EWVR)	48	36%
Noise	8	6%
Unknown	5	4%

Following a maximum of 10 alternating clockwise and counterclockwise passes through the tilt, those gates that cannot be dealiased are deleted and dealiasing is then complete for that tilt. Occasionally, isolated echoes are encountered in which none of the gates can be dealiased to within $0.5V_n$ of the auxiliary wind information. 4DD makes no attempt to interpret these echoes further, and they are deleted to prevent error propagation into later volumes.

4. Algorithm performance

4DD operated in real time on C-band Doppler velocity measurements from the Swiss Monte Lema radar throughout the entire 2-month duration of MAP. The time required to process the 20-tilt volumes on a Sun Ultra 10 workstation (300 MHz UltraSPARC-IIi, 4.3 GB HDD, 128 MB DRAM) ranged from approximately 5 to 20 s, depending on the quantity of valid gates contained in the volume. This efficiency could have been greatly improved by reading/writing a more compact radar format than Universal Format (Barnes 1980).

The Monte Lema radar is located at 1.6 km mean sea level elevation on the southern side of the European Alps where the flow and climatological precipitation are strongly influenced by orography. Monte Lema velocities pose a challenge to any dealiasing algorithm because the lowest tilts are largely attenuated by terrain clutter and fragmented by shadowing. Furthermore, with a wavelength λ of 5.515 cm and a pulse repetition frequency f of 600 s^{-1}, V_n equals just 8.27 m s^{-1} in the four lowest tilts [see Joss et al. (1998) for more details].

4DD nevertheless produced consistent and reliable results during both convective and stratiform precipitation events. This success could be attributed, in part, to the availability of wind profile estimates from an operational VAD algorithm (Germann 1999). Because the VAD algorithm is capable of producing VADs from an uncorrected radial velocity field, the wind profiles were available for nearly every volume and provided an excellent source for auxiliary wind information. However, as stated before, the VAD winds were used only when initializing the dealiasing chain and during auxiliary dealiasing. Figure 4 shows a sample 0.5° tilt dealiased by 4DD on 20 September 1999. On that day, wind speeds exceeded 30 m s^{-1} with considerable em-

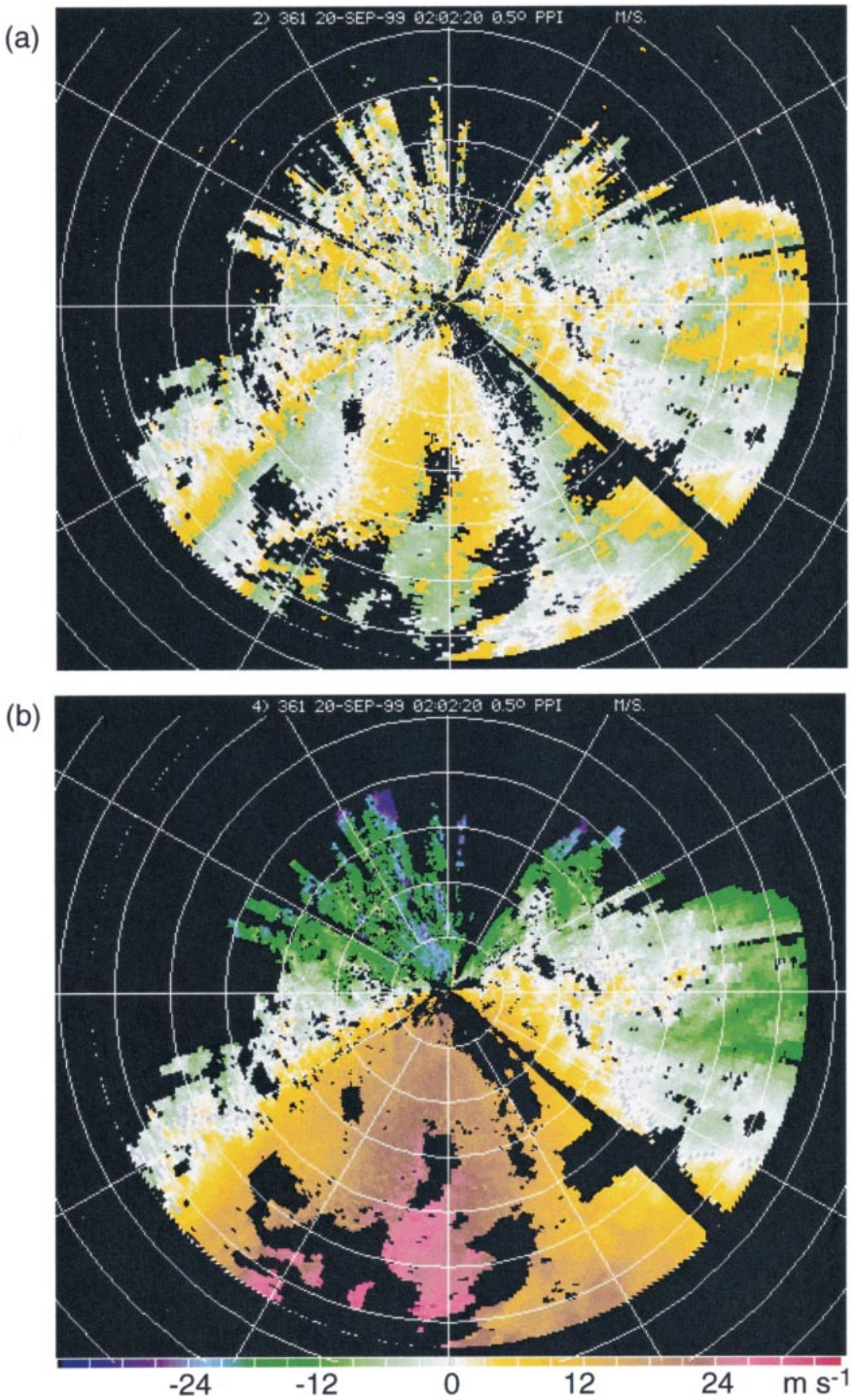

FIG. 4. A 0.5° radial velocity tilt acquired during MAP at 0202 UTC 20 Sep 1999 (a) before and (b) after automatic real-time dealiasing via 4DD. The range-ring spacing is 20 km.

bedded convection and turbulence apparent in the radar fields. Even to the trained observer, manual dealiasing of this radial velocity tilt appears nearly impossible without some knowledge of the velocity field (see Fig. 4a). However, as exhibited in Fig. 4b, it appears that 4DD correctly dealiased the noisy, doubly folded radial velocity field.

Prior to MAP, 4DD was rigorously tested on 241 volumes obtained during two complex events observed by the Monte Lema radar. The first case (3 September 1998)

exhibited embedded convection and considerable data scatter near the Alpine crest that appeared to be associated with strong turbulence. In the second case (5 September 1998), strong horizontal and vertical shear was observed in conjunction with a squall line similar to the one documented by James et al. (2000). By locating discontinuities in the radial velocity field, errors were identified and the source of error in each volume was investigated. The areal extent of the error in each tilt was also estimated and documented. Table 1 summarizes the test performance of 4DD during the two events, with a total of 241 volumes examined. Results indicate that over half (134) of the volumes contained at least one erroneous gate. On the other hand, an impressive 3993 or 93% of the 4300 tilts containing valid data were correctly interpreted by 4DD. The average number of tilts per volume containing errors was therefore 1.27 (usually in one of the lowest four sweeps where V_n was lowest). To illustrate the areal extent of these errors, the erroneous gates in the most problematic tilt in each volume covered an average of just 3% of the geographical area covered by the tilt. These statistics indicate that though the errors produced by 4DD were frequent, they were typically very localized. It should also be kept in mind that these were highly turbulent, sheared events at very low V_n and that these statistics are a pessimistic representation of the algorithm's overall performance.

Table 1 also indicates that a number of isolated radar echoes were deleted during auxiliary dealiasing (an average of one echo in every four volumes). As stated earlier, the auxiliary dealiasing routine is designed to delete echoes if none of the gates can be dealiased to within $0.5V_n$ of the corresponding gates in EWVR. The fact that so many echoes were deleted by auxiliary dealiasing is an indication that the velocity field during these high-shear events was not well approximated by a one-dimensional environmental wind profile. These results justify the need for four-dimensional dealiasing algorithms that minimize the use of auxiliary wind information.

Table 2 tallies the leading source of dealiasing error within all of the problematic radar volumes during both events (134 volumes total). The errors originated from a number of causes, the most common (54%) being strong gate-to-gate shear that was poorly resolved by V_n. In some cases, the gate-to-gate shear approached magnitudes of $2V_n$ or more, making proper dealiasing impossible by almost any means. The other major source of error (36%) was the occurrence of isolated echoes that were incorrectly interpreted by EWVR during auxiliary dealiasing. One surprising result implied from the results in Table 2 is that error propagation between successive volumes was *not* a significant source of error. Once sources of error disappeared from the radial velocity field (e.g., strong shear subsided or isolated echoes became connected with other echoes), the errors went away. Thus, the use of both vertical and temporal continuity constraints during initial dealiasing effectively mitigated error propagation.

5. Conclusions

A review of existing radial velocity dealiasing algorithms indicates that each neglects environmental wind shear in one way or another. Early dealiasing algorithms made simple assumptions about the character of the wind field (e.g., Bargen and Brown 1980). More recent schemes have relied on auxiliary information from a nearby sounding (e.g., Eilts and Smith 1990), a VAD wind profile (e.g., Bergen and Albers 1988), or a radar-generated wind model (e.g., Yamada and Chong 1999). These approaches are too simplified to operate in high-shear orographic regimes and/or at low Nyquist velocity. The extensive use of auxiliary wind information arises from the fact that these algorithms fail to incorporate the full four-dimensionality available in modern operational radar data streams.

Scaling arguments indicate that for typical mesoscale flow resolved by operational Doppler radars, the previous radar volume adequately approximates the current radial velocity field, if it is properly dealiased. Bergen and Albers (1988) produced promising test results indicating that the addition of the vertical dimension reduced the need for auxiliary wind information. Our study shows that incorporating the vertical dimension together with the time dimension helps mitigate the propagation of errors between successive volumes and effectively initializes dealiasing while minimizing the need for other wind information.

Following initial dealiasing, based on time continuity, 4DD applies azimuthal, radial, and diagonal continuity to remove local folds. The use of multiple dimensions during spatial dealiasing makes 4DD less susceptible to errors caused by strong shear and noise. The spatial dealiasing scheme in the algorithm is designed to postpone dealiasing difficult regions until the first two passes are complete. These passes are performed in alternating directions, improving the algorithm's efficiency and allowing shear zones to be approached from less complex regions on all sides. These steps make 4DD forgiving of strong shear, although excessive gate-to-gate shear approaching magnitudes of $2V_n$ may be impossible to dealias properly. Following spatial dealiasing, the algorithm then applies area averaging to evaluate remaining disconnected gates and problem areas. Because auxiliary wind information from a sounding or VAD neglects horizontal shear, it is incorporated in the final dealiasing step as a last resort when isolated echoes cannot be interpreted otherwise.

Like all dealiasing algorithms, 4DD has limitations. As a new algorithm, the sensitivities of its shear parameters are not well understood. Its performance could be improved by further testing these sensitivities and fine-tuning the parameters for a given Nyquist velocity and/or climatic regime. Another limitation is the interpre-

tation of distant isolated cells that develop or move within range of the radar, or when fast-moving highly sheared features are observed. Though vertical and temporal continuity constraints are used to mitigate errors during initial dealiasing, these scenarios sometimes prove problematic for 4DD. Further testing of 4DD's performance, especially in comparison to other dealiasing algorithms at various Nyquist velocities, is therefore warranted.

There are also a few logistical limitations associated with 4DD. The algorithm uses four-dimensional information to dealias each sweep, and therefore should operate on a continuous full-volume data stream. Whenever there are breaks in the data transmission, it relies heavily on auxiliary wind information, thus increasing the likelihood of errors in the first volume or volumes thereafter. In addition, 4DD must operate on a regular tilt sequence, beginning with the highest tilt and proceeding on down to the lowest. Otherwise, it must wait until the volume scan is complete before beginning the dealiasing sequence, resulting in a time lag that could be unfavorable for some real-time applications. 4DD also requires more memory than most algorithms because it refers to the previous radar volume and previous tilt, though this latter limitation could be remedied somewhat by storing only a fraction of the good radar gates from the previous volume and tilt in memory.

Nevertheless, 4DD performed efficiently and consistently in real time during MAP. Typical clock times on a Sun Ultra10 workstation ranged from 5–20 s, depending on the number of valid gates contained in the volume, the number of tilts, and the radar gate geometry. 4DD bench tests using WSR-88D volumes are less time efficient because the azimuth angles of WSR-88D radials vary between successive volumes and adjacent tilts, and a significant amount of processing time is spent locating the correct radial. In addition, WSR-88D radial velocity gate spacing is 0.25 km, which gives four times the resolution available in Monte Lema data.

4DD was further tested during two precipitation events over complex terrain observed by the Swiss Monte Lema radar at Nyquist velocities as low as 8.27 m s^{-1}. A total of 93% of the 4300 tilts containing valid data sustained no error. When errors occurred, they were usually very localized, resulting mainly from excessive shear and incorrect VAD-based echo interpretation. Although further research is needed to assess 4DD's effectiveness in other climatic regimes, the scheme produced promising results in a variety of meteorological conditions during MAP.

Acknowledgments. Monte Lema radar data were provided by Gianmario Galli of the Swiss Meteorological Institute (SMI). The authors appreciate the assistance and guidance provided by Jürg Joss, Gianmario Galli, and Urs Germann of SMI and by Dale Durran, Sandra Yuter, Stacy Brodzik, and Candace Gudmundson of the University of Washington. This research was supported by National Science Foundation Grants ATM-9409988 and ATM-9817700 and by Office of Naval Research Grant N00014-97-0717.

REFERENCES

Banta, R. M., 1990: The role of mountain flows in making clouds. *Atmospheric Processes over Complex Terrain, Meteor. Monogr.*, No. 45, Amer. Meteor. Soc., 229–283.

Bargen, D. W., and R. C. Brown, 1980: Interactive radar velocity unfolding. Preprints, *19th Conf. on Radar Meteorology*, Miami, FL, Amer. Meteor. Soc., 278–283.

Barnes, S. L., 1980: Report on a meeting to establish a common Doppler radar data exchange format. *Bull. Amer. Meteor. Soc.*, **61,** 1401–1404.

Bergen, W. R., and S. C. Albers, 1988: Two- and three-dimensional dealiasing of Doppler radar velocities. *J. Atmos. Oceanic Technol.*, **5,** 305–319.

Binder, P., and Coauthors, 1995: Mesoscale Alpine Programme: Design proposal. MAP Data Centre, ETH Zürich, 65 pp.

Bougeault, P., and Coauthors, 2001: The MAP special observing period. *Bull. Amer. Meteor. Soc.*, **82,** 433–462.

Browning, K. A., and R. Wexler, 1968: The determination of kinematic properties of a wind field using Doppler radar. *J. Appl. Meteor.*, **7,** 105–113.

Chong, M., and Coauthors, 2000: Real-time wind synthesis from Doppler radar observations during the Mesoscale Alpine Programme. *Bull. Amer. Meteor. Soc.*, **81,** 2953–2962.

Doviak, R. J., and D. S. Zrnić, 1993: *Doppler Radar and Weather Observations.* 2d ed. Academic Press, 562 pp.

Durran, D. R., 1986: Mountain waves. *Mesoscale Meteorology and Forecasting*, P. Ray, Ed., Amer. Meteor. Soc., 472–492.

Eilts, M. D., and S. D. Smith, 1990: Efficient dealiasing of Doppler velocities using local environment constraints. *J. Atmos. Oceanic Technol.*, **7,** 118–128.

Georgis, J.-F., F. Roux, and P. H. Hildebrand, 2000: Observation of precipitating systems over complex orography with meteorological Doppler radars: A feasibility study. *Meteor. Atmos. Phys.*, **72,** 185–202.

Germann, U., 1999: Vertical wind profile by Doppler radars. *MAP Newsletter*, No. 11, 6–7. [Available from Swiss Meteorological Institute, CH-8044 Zurich, Switzerland.]

Hennington, L., 1981: Reducing the effects of Doppler radar ambiguities. *J. Appl. Meteor.*, **20,** 1543–1546.

Houze, R. A., Jr., 1993: *Cloud Dynamics.* Academic Press, 573 pp.

James, C. N., S. R. Brodzik, H. Edmon, R. A. Houze Jr., and S. E. Yuter, 2000: Radar data processing and visualization over complex terrain. *Wea. Forecasting*, **15,** 327–338.

Jing, Z., and G. Wiener, 1993: Two-dimensional dealiasing of Doppler velocities. *J. Atmos. Oceanic Technol.*, **10,** 798–808.

Joss, J., and Coauthors, 1998: Operational use of radar for precipitation measurements in Switzerland. Final Rep., NRP 31, ETH Zürich, 108 pp.

Merritt, M. W., 1984: Automatic velocity dealiasing for real-time applications. *Proc. 22d Conf. on Radar Meteorology*, Zurich, Switzerland, Amer. Meteor. Soc., 528–533.

Ray, P., and C. Ziegler, 1977: Dealiasing first moment Doppler estimates. *J. Appl. Meteor.*, **16,** 563–564.

Schär, C., and D. R. Durran, 1997: Vortex formation and vortex shedding in continuously stratified flows past isolated topography. *J. Atmos. Sci.*, **54,** 534–554.

Smith, R. B., 1979: The influence of mountains on the atmosphere. *Advances in Geophysics*, Vol. 21, Academic Press, 87–230.

Whiteman, C. D., 1990: Observations of thermally developed wind systems in mountainous terrain. *Atmospheric Processes over Complex Terrain, Meteor Monogr.*, No. 45, Amer. Meteor. Soc., 5–42.

Yamada, Y., and M. Chong, 1999: VAD-based determination of the Nyquist interval number of Doppler velocity aliasing without wind information. *J. Meteor. Soc. Japan*, **77,** 447–457.